Interspecific competition and protistan grazing affect the coexistence of freshwater betaproteobacterial strains

Salcher, Michaela M ; Ewert, Claudia ; Šimek, Karel ; Kasalický, Vojtěch ; Posch, Thomas

Abstract: The competitive strength of four cosmopolitan freshwater betaproteobacterial isolates was investigated in the presence or absence of bacterivorous flagellates during continuous cultivation in artificial minimal medium at two dilution rates. Bacteria reached similar abundance and growth rate in monocultures, but in co-cultures, two strains (Acidovorax sp. and Massilia sp.) displayed significantly higher numbers and growth rates. These potential cross-feeding benefits were also supported by a high nutritional versatility of the two strains. In contrast, Hydrogenophaga sp. was seemingly less competitive or even inhibited by co-cultivation, and Limnohabitans planktonicus displayed striking abundance fluctuations. The latter two strains were least versatile in the uptake of different carbon sources and thus suffered more from interspecific competition. Moreover, remarkable strain-specific responses appeared when bacteria experienced increasing loss rates due to grazing and/or raised dilution rates. Limnohabitans planktonicus developed no successful defence strategy and was close to extinction. Massilia sp. formed grazing-resistant filaments exclusively at low dilution, but was highly reduced at increased flow-through. Acidovorax sp. was selectively ingested, but compensated grazing losses with accelerated growth rates and formed (co-)aggregates together with Hydrogenophaga sp. to escape predation at high flow-through. These species-specific interactions, growth responses and defence strategies strongly modulate mixed microbial assemblages and the microbial food web.

DOI: https://doi.org/10.1093/femsec/fiv156

Interspecific competition and protistan grazing affect the coexistence of freshwater betaproteobacterial strains

Michaela M. Salcher[1, 2]*, Claudia Ewert[2], Karel Šimek[1], Vojtěch Kasalický[1], Thomas Posch[2]

[1]Biology Centre CAS, Institute of Hydrobiology, České Budějovice, Czech Republic

[2]Limnological Station, University of Zurich, Kilchberg, Switzerland

Intended as research article in FEMS Microbial Ecology

Keywords: Betaproteobacteria, chemostat, co-cultivation, flagellate selective bacterivory, interspecific competition, synergistic cooperation

Running head: Competition and grazing affect growth of Betaproteobacteria

* Corresponding author: Michaela M. Salcher, Biology Centre CAS, Institute of Hydrobiology, Na Sádkách 7, 370 05 České Budějovice, Czech Republic.

E-mail: michaelasalcher@gmail.com

The authors declare no conflict of interest.

Abstract

The competitive strength of four cosmopolitan freshwater betaproteobacterial isolates was investigated in presence or absence of bacterivorous flagellates during continuous cultivation in artificial minimal medium at two dilution rates. Bacteria reached similar abundances and growth rates in monocultures, however, in co-cultures, two strains (*Acidovorax* sp. and *Massilia* sp.) displayed significantly higher numbers and growth rates. These potential cross-feeding benefits were also supported by a high nutritional versatility of the two strains. In contrast, *Hydrogenophaga* sp. was seemingly less competitive or even inhibited by co-cultivation, and *Limnohabitans planktonicus* displayed striking abundance fluctuations. The latter two strains were least versatile in the uptake of different carbon sources and thus suffered more from interspecific competition. Moreover, remarkable strain-specific responses appeared when bacteria experienced increasing loss rates due to grazing and/or raised dilution rates. *L. planktonicus* developed no successful defence strategy and was close to extinction. *Massilia* sp. formed grazing resistant filaments exclusively at low dilution, but was highly reduced at increased flow-through. *Acidovorax* sp. was selectively ingested, but compensated grazing losses with accelerated growth rates and formed (co-)aggregates together with *Hydrogenophaga* sp. to escape predation at high flow-through. These species-specific interactions, growth responses and defence strategies strongly modulate mixed microbial assemblages and the microbial food web.

Introduction

The pelagic microbial community of freshwater lakes is composed of several hundreds to thousands species (Newton *et al.* 2011, Bižić-Ionescu *et al.* 2014, Llirós *et al.* 2014) that co-exist due to ecological niche differentiation (Salcher *et al.* 2013) and transitions from dormancy to activity (Jones and Lennon 2010). In nature, microbes tightly interact with each other and with other members of the aquatic food web. Individual bacteria are permanently facing inter- and intraspecific competition for limiting resources, however, cross-feeding on products released by other microbes might also significantly accelerate growth of distinct species (i.e., syntrophy; Turner *et al.* 1996, Šimek *et al.* 2010, Lawrence *et al.* 2012). Simultaneous to resource competition, planktonic prokaryotes are top-down controlled by bacterivorous protists, with highly species-specific impacts on both predator and prey levels (Pernthaler 2005, Šimek *et al.* 2010, Šimek *et al.* 2013). Different defence mechanisms against high levels of grazing have been described in laboratory and field experiments. Prokaryotes of very small or large size seem to be protected from predation by size-selectively feeding protists (Jürgens and Matz 2002), and several bacterial taxa showed a high morphological plasticity and formed, e.g., inedible filaments in the presence of bacterivores (Hahn and Höfle 1998, Corno and Jürgens 2006). Also the formation of microcolonies or (co-)aggregates proofed to be a highly efficient grazing protection (Jürgens and Matz 2002, Pernthaler 2005). Even if ingested, some bacteria might not be digested or are of too poor food quality to promote the growth of flagellates (Šimek *et al.* 2013). Moreover, some microbes follow a so-called opportunistic life strategy, i.e., they can compensate high grazing losses by increased growth rates (Šimek *et al.* 2005, Salcher 2014), and thus, contribute disproportionally to the carbon flow to higher trophic levels (Neuenschwander *et al.* 2015). An example for such opportunists can be found among the genus *Limnohabitans*

(Betaproteobacteria) that is selectively ingested by protists (Jezbera *et al.* 2006), but high grazing losses are counterbalanced by high growth rates (Šimek *et al.* 2005).

Betaproteobacteria are ubiquitous in freshwaters and frequently dominate the assemblage (Newton *et al.* 2011, Jezbera *et al.* 2012). Members of five families of Betaproteobacteria are highly abundant in different freshwater systems (Newton *et al.* 2011): Alcaligenaceae, Burkholderiaceae, Comamonadaceae, Methylophilaceae, and Oxalobacteraceae, with Comamonadaceae being most diversified. Burkholderiaceae and Methylophilaceae are both represented by one dominant genus in freshwaters (i.e., *Polynucleobacter* (Hahn *et al.* 2012) and '*Ca*. Methylopumilus' (Salcher *et al.* 2015)). Within Comamonadaceae, *Limnohabitans* spp. are highly abundant and well-studied both in nature and culture (Šimek *et al.* 2005, Kasalický *et al.* 2013, Šimek *et al.* 2013), however, less is known about the autecology of other taxa, except for their occurrence in different lakes (Parveen *et al.* 2011, Paver *et al.* 2013, Salcher *et al.* 2013). Freshwater Oxalobacteraceae and Alcaligenaceae are even less explored, but some genera (e.g., *Massilia*) seem to be of high relevance during cyanobacterial blooms (Bižić-Ionescu *et al.* 2014) or after rain events (Peter *et al.* 2014).

We studied four betaproteobacterial strains isolated from the pelagic realm of freshwaters in more detail: Three strains (*Acidovorax* sp. MMS1-28, *Hydrogenophaga* sp. EEcy4, and *Limnohabitans planktonicus* II-D5^{T}) are affiliated with Comamonadaceae, and *Massilia* sp. MMS1-16 is a member of Oxalobacteraceae (Fig. S1). All four genera are abundant in various lake types, being seemingly associated with primary producers (Jezbera *et al.* 2012, Paver *et al.* 2013, Bižić-Ionescu *et al.* 2014, He *et al.* 2014). We explored the interaction of these four strains in a series of experiments in the presence or absence of competitors and predators. We hypothesized that (i) some strains might profit from co-cultivation due

to syntrophic or other synergistic effects, while (ii) isolates with a low nutritional versatility might suffer more from interspecific competition. Further, (iii) we expected to detect differential responses to high grazing activity by bacterivorous flagellates, and (iv) to identify potential opportunistic strategies as described for *Limnohabitans* sp. also among other Betaproteobacteria.

Material and Methods

Isolation and classification of bacterial strains

Betaproteobacterial strains *Massilia* sp. MMS1-16 (MAS) and *Acidovorax* sp. MMS1-28 (ACIDO) were isolated by dilution to extinction (Salcher *et al.* 2015) using filtered and autoclaved lake water from Lake Zurich (5 m depth, 19 August 2010) amended with NH_4Cl (1 µM), K_2HPO_4 (0.1 µM), amino acids (arginine, glutamate, glutamine, glycine, and methionine, 0.1 µM), and other carbon compounds (D-glucose, D-ribose, pyruvate, glycerol, N-acetylglucosamine, 0.0002% final concentration). The strain *Hydrogenophaga* sp. EEcy4 (HYD) was isolated on agar plates interspersed with cryptophytes, i.e., 12 ml of a fresh culture of *Cryptomonas* sp. and 1 g yeast extract were added to 1 l of carbon-free artificial lake water (ALW) agar (Zotina *et al.* 2003). Isolates were further purified on R2A plates (Reasoner and Geldreich 1985), and DNA of single colonies was isolated with the GenEluteTM Bacterial Genomic DNA Kit (Sigma). The 16S rRNA encoding genes were sequenced with general bacterial primers GM3f, GM1f, and GM4r, (Muyzer *et al.* 1995), according to standard protocols. Partial sequences were assembled with the software DNA baser v3.5.0 (Heracle BioSoft), aligned with the SINA web aligner (www.arb.silva.de), and imported to ARB (Ludwig *et al.* 2004) using the SILVA database SSU Ref 119 (Pruesse *et al.* 2007). A maximum likelihood tree of isolates and their closest relatives (Fig. S1) was calculated on a dedicated web server with

123 the GTR-GAMMA model (Stamatakis *et al.* 2005). Almost full-length 16S rDNA
124 sequences of *Massilia* sp. MMS1-16, *Acidovorax* sp. MMS1-28, and
125 *Hydrogenophaga* sp. EEcy4 were deposited to Genbank with accession numbers
126 KM236688-KM236690. Furthermore, *Limnohabitans planktonicus* II-D5^T (LIM) (Acc.
127 FM165535, Kasalický *et al.* 2010) was used for the experiments.
128
129 **Metabolic capability tests**
130 All four bacterial strains were tested for their metabolic capabilities with BioLog
131 Microarrays PM1 plates (BioLog, Hayward, USA) using carbon-free ALW (Zotina *et*
132 *al.* 2003) as a medium. Growth was monitored automatically with an absorption
133 microplate reader (Spectra Max 190, Molecular Devices) at 600 nm with
134 measurements taken every 15 min for one week. Differences in OD_{600} were scored
135 as highly positive growth (++, >180% of control), positive growth (+, 50-180% of
136 control), weak growth (w, 10-50% of control), no growth (0, -20-10% of control) or
137 inhibition of growth (-, <-20% of control).
138
139 **Batch culture experiments**
140 All four bacterial strains were grown in triplicated monocultures in ALW
141 amended with yeast extract, casein hydrolysate, and starch (5 mg l^{-1} each) in batch
142 culture until bacteria reached stationary phase (after 4 days). Subsamples were
143 taken approximately every 12 h, fixed with formaldehyde and evaluated by flow
144 cytometry and microscopy (see below).
145
146 **Continuous cultivation (chemostat) set-up and sampling**
147 The chemostat was built in a climatic chamber and operated at 20°C in the
148 dark. The system consisted of two parallel set-ups (Fig. S2), each composed of one

149 medium vessel (10 l) and three parallel cultivation vessels (780 ml). Defined volumes
150 of media were continuously transported to cultivation vessels via peristaltic pumps
151 (Ismatec, Switzerland). Special pear-shaped bacterial traps were used to disrupt the
152 flow-line from media to the cultivation vessels, avoiding a possible upstream
153 migration of bacteria. One set-up was run at a dilution rate of 0.3 d^{-1} (slow variant),
154 the second at a dilution rate of 1 d^{-1} (fast variant). All cultivation vessels were aerated
155 from the bottom (see Fig. S2) by sterile filtered air (Sartorius Midisart2000). Through
156 this kind of aeration, we obtained also a gentle mixing of the systems. The system
157 was tested for two weeks with autoclaved distilled water to check for stability of
158 dilutions rates and tightness of connections. Before the experiment was started, the
159 whole set-ups were autoclaved. Bacteria were pre-grown in ALW amended with
160 yeast extract, casein hydrolysate, and starch (5 mg l^{-1} each), which was also the
161 medium used for the chemostat. On the first day, cultivation vessels were filled from
162 the medium vessels with 500 ml medium. Bacterial strains were inoculated with initial
163 concentrations of approx. 5 x 10^4 cells ml^{-1} each. Peristaltic pumps were stopped for
164 12 h to allow for a modest growth of bacteria, thereafter, peristaltic pumps were
165 started, running at the two dilution rates mentioned above. After a stabilization of
166 bacterial numbers at t_{72} h, the bacterivorous flagellate *Poterioochromonas*
167 *malhamensis* DS (originally classified as Ochromonas sp. DS; Hahn and Höfle 1998)
168 was inoculated in 4 vessels (two slow and two fast variants, Fig. S2) at a
169 concentration of 0.3 x 10^4 cells ml^{-1}. Vessels S1 & F1 served as control variants.
170 Samples (40 ml) were taken approximately every 12 h with sterile syringes to
171 avoid any organismic contamination. Subsamples were fixed with formaldehyde (2%
172 f. c.) for the determination of bacterial parameters. Additional subsamples were fixed
173 with lugol's solution (0.5% f. c.), followed by formaldehyde (2% f. c.), and decolorized
174 with several drops of sodium thiosulfate. This fixation protocol was proposed to

assure the integrity of flagellates' food vacuoles (Sherr and Sherr 1993). Unfixed subsamples were taken at four different time points for a determination of individual grazing rates using fluorescently labeled bacteria (FLBs, see below).

Total bacterial numbers and biomass, abundances of flagellates, filamentous bacteria, and bacterial aggregates

An inFlux V-GS cell sorter (Becton Dickinson) equipped with a UV (355 nm) laser was used for the enumeration of single celled bacteria. One ml aliquots were stained with 4',6-diamidino-2-phenylindole (DAPI, 1 µg ml^{-1} f. c.), and scatter plots of DAPI fluorescence vs. 90° light scatter were analyzed with the custom-made software JoFlow 1.0a (Villiger, unpubl.).

Subsamples of 0.2-4 ml were stained with DAPI (1 µg ml^{-1} f. c.), and filtered onto black polycarbonate filters (0.22 µm or 1 µm pore size, Sartorius, for bacteria and flagellates, respectively). Flagellates, filamentous bacteria, and bacterial aggregates were counted with a Zeiss Microscope (Zeiss AxioImager.M1) at a magnification of 400x. Twenty to 60 microscopic fields were inspected for each preparation corresponding to 17-673 flagellates, 3-138 filaments, and 4-147 aggregates per sample, depending on their actual density.

Total bacterial biomass was quantified with image analysis. Briefly, 15-20 images of bacteria were recorded with a CCD camera (Vosskühler) and an 100x oil immersion objective, and processed with the image analysis software LUCIA (Laboratory Imaging, Prague). The macro described in Posch et al. (2009) was used for determining bacterial cell volumes. Bacterial cellular carbon content was calculated using the formula developed by Loferer-Krößbacher et al (1998) and Posch et al. (2001):

$$CC = 218*V^{0.86}$$

where CC is cellular carbon content (fg C) and V is bacterial cell volume (μm^3). Bacterial biomass was estimated by multiplying carbon content with total bacterial abundance.

Quantification of individual bacterial strains

The four bacterial strains were distinguished by using specific oligonucleotide probes targeting the 16S rRNA; the probe design was conducted with the software ARB (Ludwig *et al.* 2004). We used either DOPE-FISH (fluorescence in situ hybridization with double labeled probes; Stoecker *et al.* 2010) or CARD-FISH (fluorescence in situ hybridization combined with catalyzed reporter deposition; Pernthaler *et al.* 2002) for a quantification of strains (Table 1). Briefly, 0.2-4 ml subsamples were filtered onto white polycarbonate filters (0.22 µm pore size, Millipore), rinsed with distilled water, air dried, and stored at -20°C until further processing. All filters were predigested with lysozyme (10 mg ml^{-1}) for 30 min to enhance probe accessibility. DOPE-FISH was carried out with oligonucleotide probes double-labeled with either Cy3 or fluorescein and CARD-FISH was done with tyramides labeled with fluorescein (Table 1).

Filter sections were counterstained with DAPI (1 µg ml^{-1} f. c.), pictures were taken with a fully automated epifluorescence microscope (Zeder and Pernthaler 2009) and analyzed with the freeware image analysis software ACME-tool (technobiology.ch). At least 10 high quality images or > 1000 DAPI stained bacteria were evaluated per sample.

Quantification of individual grazing rates

All four strains were used in short-term direct uptake experiments as fluorescently labeled bacteria (FLB; Sherr and Sherr 1993) to quantify the strain-

specific grazing rates of *P. malhamensis.* Briefly, each strain was pre-grown to high densities and concentrated by centrifugation (5000 x g, 30 min). Bacteria were heat killed and stained with 5-([4,6-dichlorotriazine-2-yl]amino) fluorescein (DTFA) according to Šimek et al. (1997). Uptake experiments were performed at 4 time points, i.e., at t_{86}, t_{110}, t_{158}, and t_{182} h. Fresh samples were taken from the different vessels containing grazers and each stained strain was added at concentrations corresponding to 14-36% of total bacterial numbers. Subsamples (5 ml) were taken after 15 min and 30 min, fixed with lugol's solution (0.5% f. c.), followed by formaldehyde (2% f. c.) and decolorized with several drops of sodium thiosulfate (Sherr and Sherr 1993). Samples were stained with DAPI (1 µg ml^{-1} f. c.), filtered onto black 1 µm pore-size filters (Sartorius) and inspected via epifluorescence microscopy (Zeiss AxioImager.M1) at a magnification of 1000x. At least 100 flagellate cells were checked for FLB uptake in each sample. Uptake rates were calculated by multiplying average numbers of FLB per flagellate cell with uptake time and were corrected for the actual amounts of FLB added in the different treatments. A linear interpolation between the measured values was applied for those sampling dates where no direct FLB uptake was determined. The calculated average daily uptake rates were multiplied with the *in situ* abundances of *P. malhamensis* in the different vessels to estimate total grazing rates (TGR, bacteria ml^{-1} d^{-1}) on the respective bacterial strains. Selectivity indices (SI) were calculated according to Jezbera et al. (2006) by dividing the relative abundance (%) of incorporated bacteria of each strain with their actual relative abundance in the chemostats.

Calculation of individual loss and growth rates

Net growth rates (µ*N*) per day (d^{-1}) of different strains were determined with the following formula:

253 $$\mu N = \frac{ln(\frac{Nt_1}{Nt_0})}{t_1 - t_0}$$

254 where Nt_0 and Nt_1 are the numbers of bacteria (bacteria ml^{-1}) on two consecutive
255 sampling dates, t_0 and t_1 (d). Grazing induced loss rates (g) per day (d^{-1}) of different
256 strains were calculated with the formula:

257 $$g = ln\frac{N + TGR}{N}$$

258 where N is the actual bacterial abundance (bacteria ml^{-1}) and TGR is the actual total
259 grazing rate (bacteria ml^{-1} d^{-1}). Gross growth rates (μB) per day (d^{-1}) of different
260 strains was calculated with the equation:

261 $$\mu B = \mu N + g + D$$

262 where D is the dilution rate of chemostat per day (d^{-1}).

263

264 **Statistical analyses**

265 All data was log(x+1) transformed before statistical analyses to ensure normal
266 distribution. Cell densities and growth rates of different strains were tested for
267 significant differences in monocultures versus co-cultures (t_{72} h) and with versus
268 without predators (t_{254} h) by two-sample Student's t-tests. Resource partitioning of the
269 four strains was tested by agglomerative hierarchical clustering based on similarities
270 (unweighted pair-group average of Pearson's correlation coefficients) of their growth
271 on 95 different carbon sources (see above). Additionally, a principle component
272 analysis (based on Pearson's correlation coefficients) was carried out to display
273 uptake patterns. All analyses were performed with the Microsoft EXCEL add-in
274 program XLSTAT (www.xlstat.com).

275

276

Results and Discussion

Synergistic effects and interspecific competition in co-cultures

Bacteria reached comparable maximal abundances (1.6–6.5 x 10^6 cells ml^{-1}) and growth rates (3.4–4.2 d^{-1}) when grown separately in batch cultures (Figs. 1, 2). Interspecific interaction was studied in triplicated co-cultures in continuous cultivation, modulated by two different dilution rates (slow variant: 0.3 d^{-1}, fast variant: 1 d^{-1}) and by absence or presence of the bacterivorous flagellate. Total bacterial abundances (i.e., the accumulated numbers of the four strains) and maximal growth rates were significantly higher in co-cultures compared to monocultures (Tables S1, S2, Fig. S3). Synergistic interactions between different microbes in co-cultures typically result in a better exploitation of mixed substrates and nutrients, as can be found in every natural system (Kovárová-Kovar and Egli 1998, Tan *et al.* 2015). However, there was no difference in maximal numbers between the two dilution rates, while slightly higher gross growth rates were recorded in the version with high flow-through.

We observed striking species-specific differences in mono- and co-cultures: MAS reached more than six-fold higher abundances at both dilution rates without predators and also ACIDO were growing to significantly higher numbers (Fig. 1, Table S1). Both strains displayed significantly higher growth rates in the co-cultures compared to monocultures (Fig. 2, Table S2). In contrast, HYD reached significantly lower maximal numbers and growth rates in co-cultures (i.e., 45% and 24% of cell yields in the slow and fast variants, respectively), while LIM displayed remarkable abundance fluctuations, but no significant differences could be detected between any of the treatments (Figs. 1, 2, Tables S1, S2).

All four strains were tested for their metabolic capabilities with BioLog PM1 plates and showed distinct patterns of resource partitioning (Figs. 3, S4, Table S3). Only nine of the 95 offered carbon sources supported the growth of all four taxa, and

several substrates were exclusively used by the individual strains (6, 8, 5, and 9 substrates for ACIDO, MAS, HYD, and LIM, respectively, Fig. S4). Resource partitioning of different amino acids, sugars, and carboxylic acids has also been described for different betaproteobacterial populations in Lake Zurich, the origin of most isolates (Salcher *et al.* 2013). MAS and ACIDO displayed similar usage of carbon sources ($r = 0.362$, $p < 0.001$), while LIM and HYD were significantly different from the others. MAS and ACIDO were most versatile in the uptake of different carbon sources (52 and 54 substrates, respectively, Fig. 3, Table S3), pointing to competitive advantages and possible syntrophic cross-feeding benefits (Turner *et al.* 1996, Kovárová-Kovar and Egli 1998, Lawrence *et al.* 2012). Such cooperative adaptations typically evolved more frequently between highly related genotypes that share metabolic capabilities (Mitri and Foster 2013), such as MAS and ACIDO (Fig. 3). Metabolic dependencies and metabolite exchanges of co-occurring microbes seem to be especially important under oligotrophic conditions such as in freshwater lakes (Zelezniak *et al.* 2015). As we used a relatively nutrient and substrate poor medium to mimic natural conditions, metabolic interactions like cross-feeding might have played a major role in modifying the outcome of our experiments. HYD and LIM exploited only 36 and 35 substrates, respectively, and performed correspondingly less well in co-cultures, indicating negative effects of interspecific competition. Moreover, growth of HYD was inhibited by 14 substrates, thus, the strain might even have been inhibited by specific substrates produced in co-cultures if their concentrations were high enough (Fiegna *et al.* 2015).

Impact of grazing by flagellates

The combined effects of predation and competition were investigated by addition of the mixotrophic chrysophyte *Poterioochromonas malhamensis* strain DS

as a predator. This ubiquitous bacterivorous flagellate is a frequently used model organism with high clearance rates and size selective predation (Hahn and Höfle 1998, Posch *et al.* 1999, Jürgens and Matz 2002). Flagellates reached higher densities in the slow than in the fast variants (Fig. 1), most likely because a dilution rate of 1 d^{-1} is already close to their maximal growth rates achievable on the given combination of food items (Šimek *et al.* 2006, Šimek *et al.* 2013). Bacteria stabilized to comparable total numbers and biomasses at both dilution rates after an initial drop during the highest bacterivory phase (Fig. S3, Table S1). This was reached by a strong increase in growth rate (~48 h after the addition of the bacterivore) with maxima comparable to or even higher than the initial pre-stabilization period of the chemostat (Fig. 2, Fig. S3). Dilution-rate dependent significant differences were observed for MAS with stable cell numbers in the slow variants compared to a constant decline in the fast variants (Table S1). ACIDO and HYD could retain high abundances in both variants after a short drop during highest bacterivory, while LIM were strongly reduced and almost extinct at the end of the experiment (Fig. 1).

Strain-specific grazing rates were determined in short-term uptake experiments with fluorescently labelled bacteria (Fig. S5). Highest total grazing rates were recorded in the low-dilution variant three days after the introduction of flagellates (10 x 10^6 cells ml^{-1} d^{-1} at t_{158} h; Fig. S6), while grazing rates were lower in the fast variant and their maximum occurred earlier (7.8 x 10^6 cells ml^{-1} d^{-1} at t_{110} h). These grazing rates are within the range of published values for *P. malhamensis* DS and natural protistan communities (Posch *et al.* 1999, Šimek *et al.* 2005, Jezbera *et al.* 2006). ACIDO were the most favourable prey for flagellates with total grazing rates of up to 8.8 x 10^6 cells ml^{-1} d^{-1} (Figs. 4, S5, S6). Selectivity indices were always >1 (i.e., positive selection) with values up to 14 and these microbes accounted for the majority of ingested cells in all cases (53 – 86%). Nevertheless, ACIDO obviously

355 compensated high loss rates by enhanced growth rates, a strategy previously
356 described for planktonic *Limnohabitans* spp. (Šimek *et al.* 2005). HYD displayed the
357 lowest selectivity indices (0.1 – 1.1, i.e. strong negative to neutral selection, Fig. 4)
358 and were least ingested by *P. malhamensis*, therefore they could retain high
359 densities in both variants. MAS and LIM showed intermediate grazing losses and
360 selectivity indices. MAS was more ingested in the fast variant with a selectivity index
361 of up to 5.8 (positive selection) compared to 0.5 – 0.8 (negative selection) in the slow
362 variant, which might reflect the changing prey availability or prey food characteristics
363 under two different dilution rates. LIM was also slightly positively selected by
364 flagellates in the fast variant and negatively selected in the slow variant. However,
365 this strain accounted for a maximum of 29% of ingested bacteria at one time point
366 (t_{110}) in the slow variant, when all other taxa already dropped to very low densities
367 except for LIM (Figs. 1, 4). Thus, LIM also proofed to be of high food quality as
368 reported previously (Jezbera *et al.* 2006, Šimek *et al.* 2013), however, ACIDO and
369 partly also MAS were obviously a superior food source for *P. malhamensis* DS.
370
371 **Strain-specific grazing defence mechanisms**
372 Interestingly, strain-specific grazing defence mechanisms were observed at
373 different loss rates. High grazing pressure induced filamentation in two isolates (MAS
374 and ACIDO), however, only in variants with low dilution rate (Figs. 5, S6). Filament
375 formation is an effective grazing protection as these morphologies by far exceed the
376 size limit that can be handled and engulfed by flagellates (Hahn and Höfle 1998,
377 Jürgens and Matz 2002, Pernthaler 2005). Filamentous bacteria typically reach their
378 annual maximum in lakes after the phytoplankton spring bloom concomitantly with or
379 shortly after heterotrophic flagellate population peaks (Schauer *et al.* 2006, Salcher
380 *et al.* 2010, Eckert *et al.* 2012). Filamentous bacteria even seem to profit twofold from

381 the presence of bacterivorous flagellates, due to the elimination of competitors and
382 because of selective utilization of carbon sources that are egested by protists (Eckert
383 *et al.* 2013). Filaments were rare in the variants with high dilution rates; either
384 because of the lower grazing pressure therein or because of longer generation times
385 of filamentous bacteria (Hahn and Höfle 1998). The latter is supported by the
386 observation that filament numbers peaked only five days after flagellates' maxima
387 (Fig. 5). A delay in filament formation of several days after highest flagellate numbers
388 has also been reported from different lakes (Pernthaler *et al.* 2004, Eckert *et al.*
389 2012).

390 An alternative defence strategy was exclusively observed in the fast variants:
391 ACIDO and HYD formed microcolonies and co-aggregates simultaneous with highest
392 flagellates numbers and bacterivory (Figs. 5, S6). Bacterial microcolonies and
393 aggregates are protected from protistan predation because of their big size and
394 highly complex morphologies (Jürgens and Matz 2002, Pernthaler 2005). As
395 filaments and aggregates were almost absent in flagellate-free treatments (Fig. 5),
396 the formation of inedible morphologies might be triggered by chemical cues excreted
397 by *P. malhamensis*, as was also suggested for other microbes with high phenotypic
398 plasticity (Corno and Jürgens 2006, Blom *et al.* 2010). This refuge from grazing might
399 be another reason for the prevalence of ACIDO and HYD in the fast variants, as co-
400 aggregation fosters the coexistence and success of microbes under grazing pressure
401 (Corno *et al.* 2013). Consequently, ACIDO and HYD dominated the assemblage at
402 the end of the experiment, while MAS and LIM suffered from high grazing losses and
403 interspecific competition and were close to extinction in the fast variant (Fig. 1).
404 Moreover, interspecific interactions in co-aggregates seem to promote the utilization
405 of complex biopolymers and thus, increase the productivity and carbon transfer
406 efficiency in mixed cultures in the presence of flagellates (Corno *et al.* 2015).

Microbes closely related to ACIDO and HYD have been detected on lake or river snow particles (Böckelmann *et al.* 2000, Knoll *et al.* 2001, Schweitzer *et al.* 2001, Parveen *et al.* 2011), thus, they are able to grow on surfaces and form aggregates also in nature. LIM on the other side lives planktonic (Kasalický *et al.* 2010) or as epibiont on *Daphnia* sp. (Eckert and Pernthaler 2014) and does not display any marked morphological plasticity, as neither filaments nor aggregates were formed by this microbe. LIM therefore lacked a successful grazing defence and was most vulnerable to both, grazing and interspecific competition (Fig. 1).

The opportunistic lifestyle, i.e. rapid growth compensating for high mortality rates described for some *Limnohabitans* spp. in nature (Šimek *et al.* 2005), was not confirmed for the strain we used in our experiments (*Limnohabitans planktonicus* II-D5^{T} (Kasalický *et al.* 2010)). However, the genus *Limnohabitans* is very divers with five lineages and at least six sublineages (Kasalický *et al.* 2013), and *Limnohabitans planktonicus* II-D5^{T} seems to be not widely distributed in the plankton of lakes (Jezbera *et al.* 2013), but instead might have its niche as symbionts of zooplankton (Eckert and Pernthaler 2014, Peerakietkhajorn *et al.* 2015). Thus, our results cannot be easily translated to natural conditions in lakes, where other very competitive *Limnohabitans* lineages predominate (Šimek *et al.* 2005, Jezbera *et al.* 2013). Moreover, an artificial minimal medium was added with constant dilution rates in our chemostats, while in nature, conditions are typically more unstable with e.g., diurnal and seasonal fluctuations and resources are patchily distributed. In our experiments, ACIDO seemed to follow an opportunistic strategy, as its accelerated growth rates in presence of predators counterbalanced high grazing losses. The detailed response mechanisms, however, are still unclear, i.e., if ACIDO actively changed its gene expression patterns or if changed environmental conditions enabled the observed higher growth rates.

Conclusion

This study shows that single strains react differently to co-cultivation, with synergistic effects and interspecific competition acting simultaneously. Moreover, they developed species-specific and growth-rate dependent grazing-defence mechanisms if faced with high predation rates (Fig. S8). These responses point to highly species-specific interactions in mixed microbial assemblages that modulate aquatic microbial food webs, having fundamental importance for carbon flow from distinct resources through bacteria to the grazer food chain. Notably, this is currently one of the understudied topics of aquatic microbial ecology in urgent need of further investigations.

Funding

This work was supported by the Swiss National Science Foundation as part of the European Science Foundation EUROCORES Programme EuroEEFG [SNF grant number 31EE30-132771], by the Swiss National Science Foundation [SNF grant number 138473], and by the Czech Science Foundation [CSF grant number 13-00243S].

Acknowledgements

We thank E. Eckert for isolating *Hydrogenophaga* sp. EEcy4 and M. Baumgartner for sharing an axenic culture of *P. malhamensis* DS. We are also grateful to J. Pernthaler for discussion and to the helpful comments of two anonymous reviewers.

References

Bižić-Ionescu M, Amann R and Grossart H-P (2014) Massive regime shifts and high activity of heterotrophic bacteria in an ice-covered lake. *PLoS ONE* **9**: e113611.

Blom JF, Horňák K, Šimek K and Pernthaler J (2010) Aggregate formation in a freshwater bacterial strain induced by growth state and conspecific chemical cues. *Environ Microbiol* **12**: 2486-2495.

Böckelmann U, Manz W, Neu T and Szewzyk U (2000) Characterization of the microbial community of lotic organic aggregates ("river snow") in the Elbe River of Germany by cultivation and molecular methods. *FEMS Microbiol Ecol* **33**: 157-170.

Corno G and Jürgens K (2006) Direct and indirect effects of protist predation on population size structure of a bacterial strain with high phenotypic plasticity. *Appl Environ Microbiol* **72**: 78-86.

Corno G, Villiger J and Pernthaler J (2013) Coaggregation in a microbial predator-prey system affects competition and trophic transfer efficiency. *Ecology* **94**: 870-881.

Corno G, Salka I, Pohlmann K, Hall A and Grossart H (2015) Interspecific interactions drive chitin and cellulose degradation by aquatic microorganisms. *Aquat Microb Ecol* **76**: 27-37.

Eckert EM and Pernthaler J (2014) Bacterial epibionts of *Daphnia*: a potential route for the transfer of dissolved organic carbon in freshwater food webs. *ISME J* **8**: 1808-1819.

Eckert EM, Baumgartner M, Huber IM and Pernthaler J (2013) Grazing resistant freshwater bacteria profit from chitin and cell-wall derived organic carbon. *Environ Microbiol* **15**: 2019-2030.

Eckert EM, Salcher MM, Posch T, Eugster B and Pernthaler J (2012) Rapid successions affect microbial N-acetyl-glucosamine uptake patterns during a lacustrine spring phytoplankton bloom. *Environ Microbiol* **14**: 794-806.

Fiegna F, Moreno-Letelier A, Bell T and Barraclough TG (2015) Evolution of species interactions determines microbial community productivity in new environments. *ISME J* **9**: 1235-1245.

Hahn M and Höfle M (1998) Grazing pressure by a bacterivorous flagellate reverses the relative abundance of *Comamonas acidivorans* PX54 and *Vibrio* strain CB5 in chemostat coculture. *Appl Environ Microbiol* **64**: 1910-1918.

Hahn MW, Scheuerl T, Jezberova J*, et al.* (2012) The passive yet successful way of planktonic life: Genomic and experimental analysis of the ecology of a free-living *Polynucleobacter* population. *PLoS ONE* **7**: e32772.

He D, Ren L and Wu QL (2014) Contrasting diversity of epibiotic bacteria and surrounding bacterioplankton of a common submerged macrophyte, *Potamogeton crispus*, in freshwater lakes. *FEMS Microbiol Ecol* **90**: 551-562.

Jezbera J, Horňák K and Šimek K (2006) Prey selectivity of bacterivorous protists in different size fractions of reservoir water amended with nutrients. *Environ Microbiol* **8**: 1330-1339.

Jezbera J, Jezberová J, Kasalický V, Šimek K and Hahn MW (2013) Patterns of *Limnohabitans* microdiversity across a large set of freshwater habitats as revealed by reverse line blot hybridization. *PLoS ONE* **8**: e58527.

Jezbera J, Jezberová J, Koll U, Horňák K, Šimek K and Hahn MW (2012) Contrasting trends in distribution of four major planktonic betaproteobacterial groups along a pH gradient of epilimnia of 72 freshwater habitats. *FEMS Microbiol Ecol* **81**: 467-479.

Jones SE and Lennon JT (2010) Dormancy contributes to the maintenance of microbial diversity. *Proc Natl Acad Sci USA* **107**: 5881-5886.

Jürgens K and Matz C (2002) Predation as a shaping force for the phenotypic and genotypic composition of planktonic bacteria. *Antonie Van Leeuwenhoek* **81**: 413-434.

Kasalický V, Jezbera J, Šimek K and Hahn MW (2010) *Limnohabitans planktonicus* sp. nov., and *Limnohabitans parvus* sp. nov., two novel planktonic *Betaproteobacteria* isolated from a freshwater reservoir and emended description of the genus *Limnohabitans*. *Int J Syst Evol Microbiol* **60**: 2710-2714.

Kasalický V, Jezbera J, Hahn MW and Šimek K (2013) The diversity of the *Limnohabitans* genus, an important group of freshwater bacterioplankton, by characterization of 35 isolated strains. *PLoS ONE* **8**: e58209.

Knoll S, Zwisler W and Simon M (2001) Bacterial colonization of early stages of limnetic diatom microaggregates. *Aquat Microb Ecol* **25**: 141-150.
Kovárová-Kovar K and Egli T (1998) Growth kinetics of suspended microbial cells: From single-substrate-controlled growth to mixed-substrate kinetics. *Microbiol Mol Biol R* **62**: 646-666.
Lawrence D, Fiegna F, Behrends V, Bundy JG, Phillimore AB, Bell T and Barraclough TG (2012) Species interactions alter evolutionary responses to a novel environment. *PLoS Biol* **10**: e1001330.
Llirós M, Inceoğlu Ö, García-Armisen T*, et al.* (2014) Bacterial community composition in three freshwater reservoirs of different alkalinity and trophic status. *PLoS ONE* **9**: e116145.
Loferer-Krößbacher M, Klima J and Psenner R (1998) Determination of bacterial cell dry mass by transmission electron microscopy and densiometric image analysis. *Appl Environ Microbiol* **64**: 668-694.
Ludwig W, Strunk O, Westram R*, et al.* (2004) ARB: a software environment for sequence data. *Nucl Acid Res* **32**: 1363-1371.
Mitri S and Foster KR (2013) The genotypic view of social interactions in microbial communities. *Ann Rev Genet* **47**: 247-273.
Muyzer G, Teske A, Wirsen C and Jannasch H (1995) Phylogenetic relationship of *Thiomicrospira* species and their identification in deep-sea hydrothermal vent samples by denaturing gel electrophoresis of 16S rDNA fragments. *Arch Microbiol* **164**: 165-172.
Neuenschwander SM, Pernthaler J, Posch T and Salcher MM (2015) Seasonal growth potential of rare lake water bacteria suggest their disproportional contribution to carbon fluxes. *Environ Microbiol* **17**: 781-795.
Newton RJ, Jones SE, Eiler A, McMahon KD and Bertilsson S (2011) A guide to the natural history of freshwater lake bacteria. *Microbiol Mol Biol R* **75**: 14-49.
Parveen B, Reveilliez J-P, Mary I*, et al.* (2011) Diversity and dynamics of free-living and particle-associated *Betaproteobacteria* and *Actinobacteria* in relation to phytoplankton and zooplankton communities. *FEMS Microbiol Ecol* **77**: 461-476.
Paver SF, Hayek KR, Gano KA*, et al.* (2013) Interactions between specific phytoplankton and bacteria affect lake bacterial community succession. *Environ Microbiol* **15**: 2489-2504.
Peerakietkhajorn S, Kato Y, Kasalický V, Matsuura T and Watanabe H (2015) Betaproteobacteria *Limnohabitans* strains increase fecundity in the crustacean *Daphnia magna*: symbiotic relationship between major bacterioplankton and zooplankton in freshwater ecosystem. *Environ Microbiol* online early.
Pernthaler A, Pernthaler J and Amann R (2002) Fluorescence in situ hybridization and catalyzed reporter deposition for the identification of marine bacteria. *Appl Environ Microbiol* **68**: 3094-3101.
Pernthaler J (2005) Predation on prokaryotes in the water column and its ecological implications. *Nat Rev Microbiol* **3**: 537-546.
Pernthaler J, Zollner E, Warnecke F and Jurgens K (2004) Bloom of filamentous bacteria in a mesotrophic lake: Identity and potential controlling mechanism. *Appl Environ Microbiol* **70**: 6272-6281.
Peter H, Hörtnagl P, Reche I and Sommaruga R (2014) Bacterial diversity and composition during rain events with and without Saharan dust influence reaching a high mountain lake in the Alps. *Environ Microbiol Rep* **6**: 618-624.
Posch T, Franzoi J, Prader M and Salcher MM (2009) New image analysis tool to study biomass and morphotypes of three major bacterioplankton groups in an alpine lake. *Aquat Microb Ecol* **54**: 113-126.
Posch T, Loferer-Krossbacher M, Gao G, Alfreider A, Pernthaler J and Psenner R (2001) Precision of bacterioplankton biomass determination: a comparison of two fluorescent dyes, and of allometric and linear volume-to-carbon conversion factors. *Aquat Microb Ecol* **25**: 55-63.
Posch T, Šimek K, Vrba J*, et al.* (1999) Predator-induced changes of bacterial size-structure and productivity studied on an experimental microbial community. *Aquat Microb Ecol* **18**: 235-246.

Pruesse E, Quast C, Knittel K, Fuchs BM, Ludwig W, Peplies J and Glöckner FO (2007) SILVA: a comprehensive online resource for quality checked and aligned ribosomal RNA sequence data compatible with ARB. *Nucl Acid Res* **35**: 7188-7196.

Reasoner DJ and Geldreich EE (1985) A new medium for the enumeration and subculture of bacteria from potable water. *Appl Environ Microbiol* **49**: 1-7.

Salcher MM (2014) Same same but different: ecological niche partitioning of planktonic freshwater prokaryotes. *J Limnol* **73**: 74-87.

Salcher MM, Pernthaler J and Posch T (2010) Spatiotemporal distribution and activity patterns of bacteria from three phylogenetic groups in an oligomesotrophic lake. *Limnol Oceanogr* **55**: 846-856.

Salcher MM, Posch T and Pernthaler J (2013) *In situ* substrate preferences of abundant bacterioplankton populations in a prealpine freshwater lake. *ISME J* **7**: 896-907.

Salcher MM, Neuenschwander SM, Posch T and Pernthaler J (2015) The ecology of pelagic freshwater methylotrophs assessed by a high-resolution monitoring and isolation campaign. *ISME J* **9**: 2442-2453.

Schauer M, Jiang J and Hahn M (2006) Recurrent seasonal variations in abundance and composition of filamentous SOL cluster bacteria (*Saprospiraceae*, *Bacteroidetes*) in oligomesotrophic lake Mondsee (Austria). *Appl Environ Microbiol* **72**: 4704-4712.

Schweitzer B, Huber I, Amann R, Ludwig W and Simon M (2001) alpha- and beta-Proteobacteria control the consumption and release of amino acids on lake snow aggregates. *Appl Environ Microbiol* **67**: 632-645.

Sherr E and Sherr B (1993) Preservation and storage of samples for enumeration of heterotrophic protist. *Handbook of Methods in Aquatic Microbial Ecology,*(Kemp P, Sherr E, Sherr B and Cole J, ed.^eds.), p.^pp. 207-212. Lewis Publishers.

Sherr EB and Sherr BF (1993) Protistan grazing rates via uptake of fluorescently labeled prey. *Handbook of Methods in Aquatic Microbial Ecology,*(Kemp PF, Sherr BF, Sherr EB and Cole JJ, ed.^eds.), p.^pp. 695-701. Lewis Publ, Boca Raton.

Šimek K, Kasalický V, Horňák K, Hahn MW and Weinbauer MG (2010) Assessing niche separation among coexisting *Limnohabitans* strains through interactions with a competitor, viruses, and a bacterivore. *Appl Environ Microbiol* **76**: 1406-1416.

Šimek K, Hartman P, Nedoma J, Pernthaler J, Springmann D, Vrba J and Psenner R (1997) Community structure, picoplankton grazing and zooplankton control of heterotrophic nanoflagellates in a eutrophic reservoir during the summer phytoplankton maximum. *Aquat Microb Ecol* **12**: 49-63.

Šimek K, Horňák K, Jezbera J, Masin M, Nedoma J, Gasol J and Schauer M (2005) Influence of top-down and bottom-up manipulation on the R-BT065 subcluster of beta-proteobacteria, an abundant group in bacterioplankton of a freshwater reservoir. *Appl Environ Microbiol* **71**: 2381-2390.

Šimek K, Horňák K, Jezbera J*, et al.* (2006) Maximum growth rates and possible life strategies of different bacterioplankton groups in relation to phosphorus availability in a freshwater reservoir. *Environ Microbiol* **8**: 1613-1624.

Šimek K, Kasalický V, Jezbera J*, et al.* (2013) Differential freshwater flagellate community response to bacterial food quality with a focus on *Limnohabitans* bacteria. *ISME J* **7**: 1519-1530.

Stamatakis A, Ludwig T and Meier H (2005) RAxML-II: a program for sequential, parallel and distributed inference of large phylogenetic. *Concurr Comput-Pract Exp* **17**: 1705-1723.

Stoecker K, Dorninger C, Daims H and Wagner M (2010) Double labeling of oligonucleotide probes for fluorescence *in situ* hybridization (DOPE-FISH) improves signal intensity and increases rRNA accessibility. *Appl Environ Microbiol* **76**: 922-926.

Tan J, Zuniga C and Zengler K (2015) Unraveling interactions in microbial communities - from co-cultures to microbiomes. *J Microbiol* **53**: 295-305.

Turner PE, Souza V and Lenski RE (1996) Tests of ecological mechanisms promoting the stable coexistence of two bacterial genotypes. *Ecology* **77**: 2119-2129.

Zeder M and Pernthaler J (2009) Multispot live-image autofocusing for high-throughput microscopy of fluorescently stained bacteria. *Cytometry Part A* **75A**: 781-788.

Zelezniak A, Andrejev S, Ponomarova O, Mende DR, Bork P and Patil KR (2015) Metabolic dependencies drive species co-occurrence in diverse microbial communities. *Proc Natl Acad Sci USA* **112**: 6449–6454.

Zotina T, Köster O and Jüttner F (2003) Photoheterotrophy and light-dependent uptake of organic and organic nitrogenous compounds by *Planktothrix rubescens* under low irradiance. *Freshwater Biol* **48**: 1859-1872.

Figure legends:

Figure 1: Abundances of the four bacterial strains grown separately in batch cultures (A), in co-cultures in continuous cultivation (B-C), and in the presence of the bacterivorous flagellate *Poterioochromonas malhamensis* DS (D-E) with slow (B, D) and fast (C, E) dilution rates. The numbers of flagellates are shown as grey shading in D and E. ACIDO, *Acidovorax* sp. MMS1-28; MAS, *Massilia* sp. MMS1-16; HYD, *Hydrogenophaga* sp. EECy4; LIM, *Limnohabitans planktonicus* II-D5^{T}.

Figure 2: Growth and loss rates of the four bacterial strains when grown separately in batch cultures (A, D, G, J), or in co-cultures in continuous cultivation with slow (B, E, H, K) and fast (C, F, I, L) dilution rates. A-C: *Acidovorax* sp. MMS1-28; D-F: *Massilia* sp. MMS1-16; G-I: *Hydrogenophaga* sp. EECy4; J-L: *Limnohabitans planktonicus* II-D5^{T}. The grey arrows indicate the time when the bacterivorous flagellate *P. malhamensis* DS was introduced.

Figure 3: Nutritional versatility of the four strains. A: Principle component analysis biplot of uptake patterns of 95 different substrates based on Pearson's correlation coefficients displaying substrate partitioning between the four strains. B: Number of substrates that supported or inhibited the growth of individual strains. ACIDO, *Acidovorax* sp. MMS1-28; MAS, *Massilia* sp. MMS1-16; HYD, *Hydrogenophaga* sp. EECy4; LIM, *Limnohabitans planktonicus* II-D5^{T}.

Figure 4: Proportional grazing losses and selectivity indices (SI) of the four bacterial strains by the flagellate *Poterioochromonas malhamensis* DS at four selected time points in the variants with slow (A) and fast (B) dilution rates. ACIDO, *Acidovorax* sp. MMS1-28; MAS, *Massilia* sp. MMS1-16; HYD, *Hydrogenophaga* sp. EECy4; LIM, *Limnohabitans planktonicus* II-D5^{T}.

650 Figure 5: Relative abundances of filamentous bacteria and bacterial aggregates in
651 the variants with slow (A) and fast (B) dilution rates.
652

Table 1. Oligonucleotide probes targeting the 16S rRNA of the bacterial strains.

Probe	Strain	Probe sequence (5' – 3')	*E. coli* position	Label	FA%	Reference
Acido-464	*Acidovorax* sp. MMS1-28	GTA CCG TCA TGG ACC CTC TTT ATT AG	464	2 x CY3	55	This study
Mas-461	*Massilia* sp. MMS1-16	CCG TCA TTA GCC GCA GAT ATT AGC C	461	2 x FITC	55	This study
Hyd-445	*Hydrogenophaga* sp. EECy4	AAC CAG GAC CGT TTC GTT CCG	445	2 x CY3	50	This study
RBT-065	*Limnohabitans planktonicus* II-D5^T	GTT GCC CCC TCT ACC GTT	65	HRP	55	(Šimek *et al.* 2001)

2 x CY3: DOPE-FISH probes labeled with CY3; 2 x FITC: DOPE-FISH probes labeled with fluorescein; HRP: CARD-FISH with horseradish peroxidase labeled probes; FA%: Formamide concentration for stringent hybridization conditions.

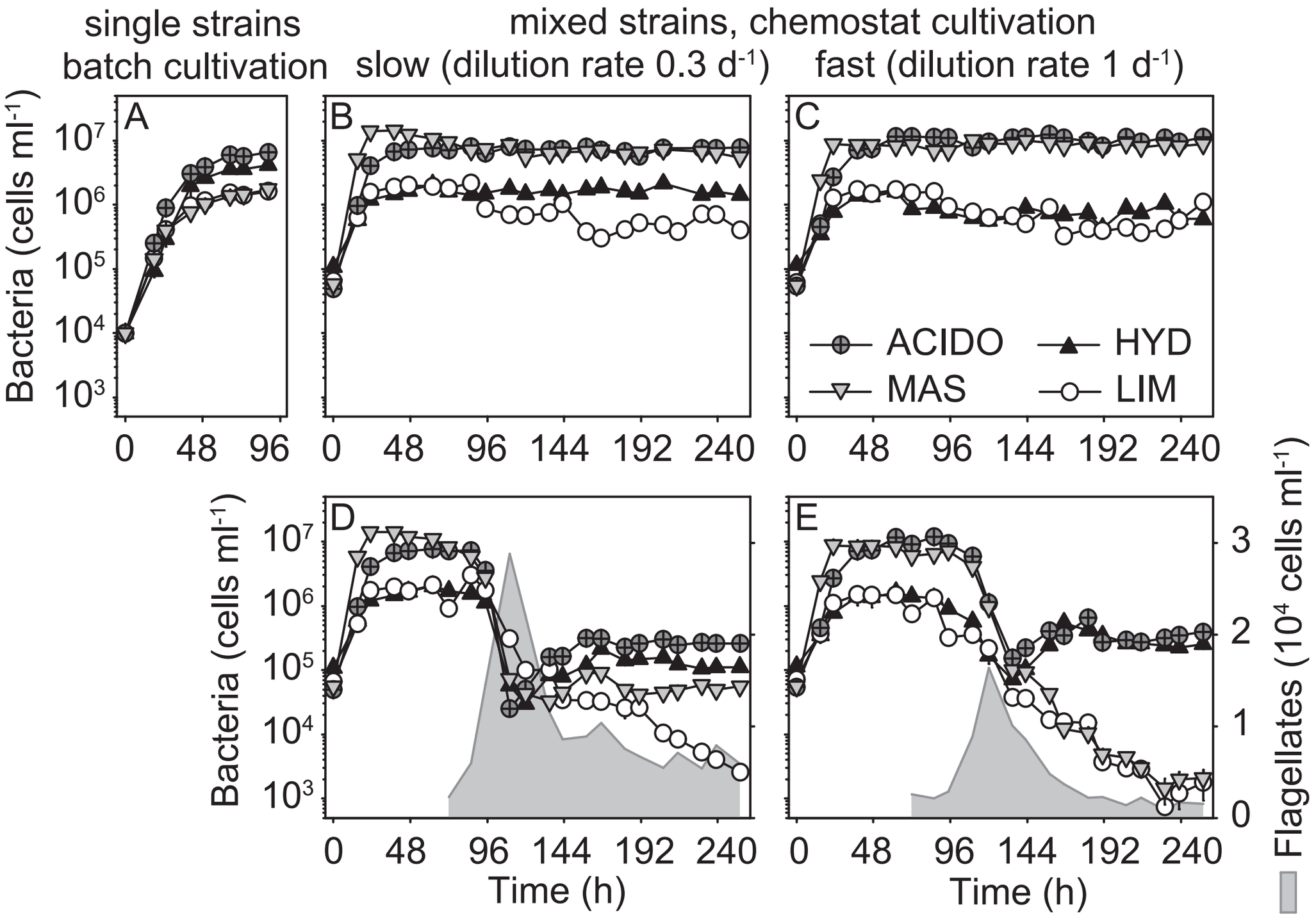
single strains
batch cultivation
mixed strains, chemostat cultivation
slow (dilution rate 0.3 d-1)
fast (dilution rate 1 d-1)
A
B
C
D
E
Bacteria (cells ml-1)
Flagellates (10^4 cells ml-1)
Time (h)
ACIDO
HYD
MAS
LIM

single strains
batch cultivation

mixed strains, chemostat cultivation
slow (dilution rate 0.3 d^{-1})

fast (dilution rate 1d^{-1})

A

B: ACIDO

C

D

E: MAS

F

G

H: HYD

I

J

K: LIM

L

gross growth rate
loss by grazing
loss by dilution

Growth rate (d^{-1}), loss rate (d^{-1})

8
4
0
-4

0
48
96
144
192

Time (h)

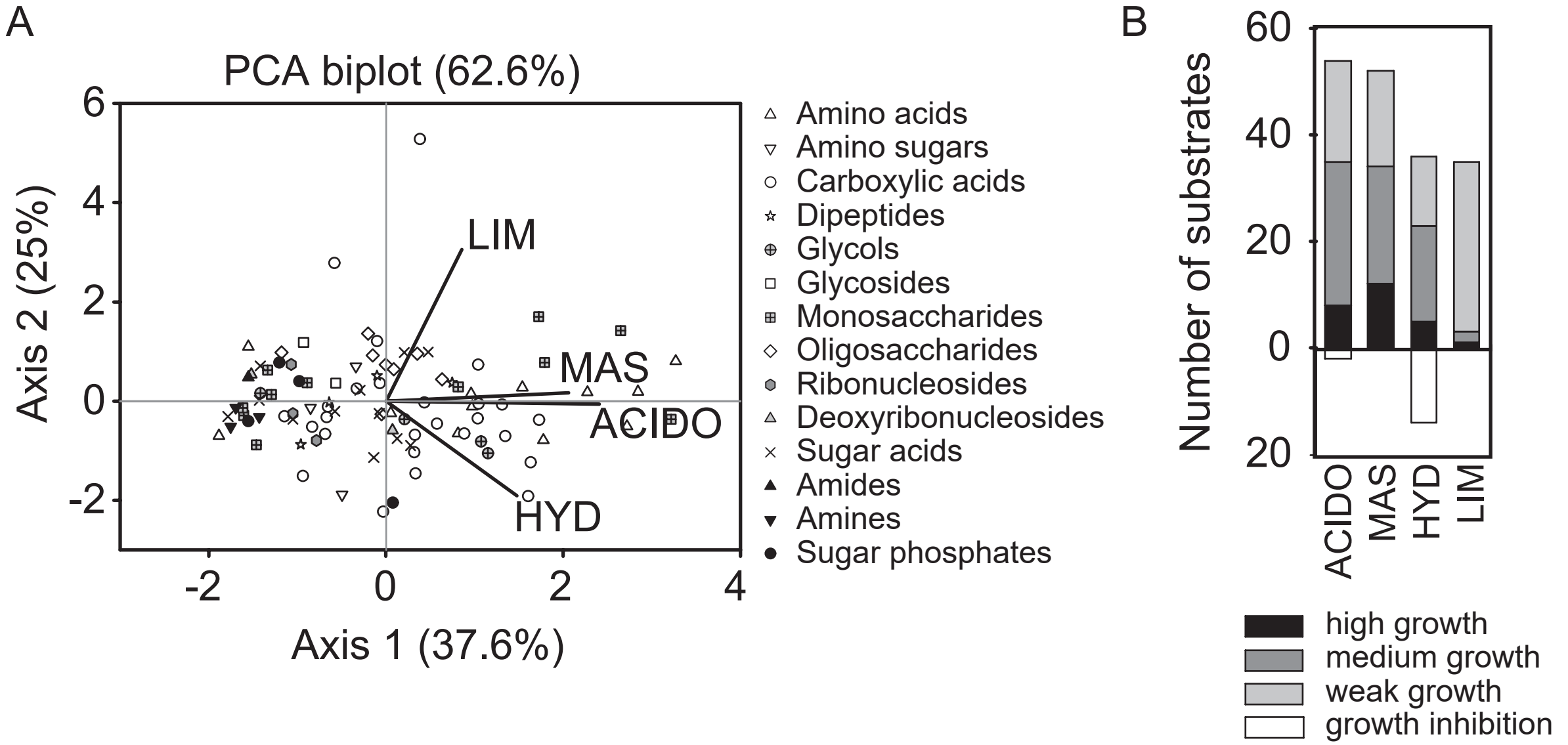
A
PCA biplot (62.6%)
Axis 2 (25%)
Axis 1 (37.6%)
LIM
MAS
ACIDO
HYD
Amino acids
Amino sugars
Carboxylic acids
Dipeptides
Glycols
Glycosides
Monosaccharides
Oligosaccharides
Ribonucleosides
Deoxyribonucleosides
Sugar acids
Amides
Amines
Sugar phosphates
B
Number of substrates
ACIDO
MAS
HYD
LIM
high growth
medium growth
weak growth
growth inhibition

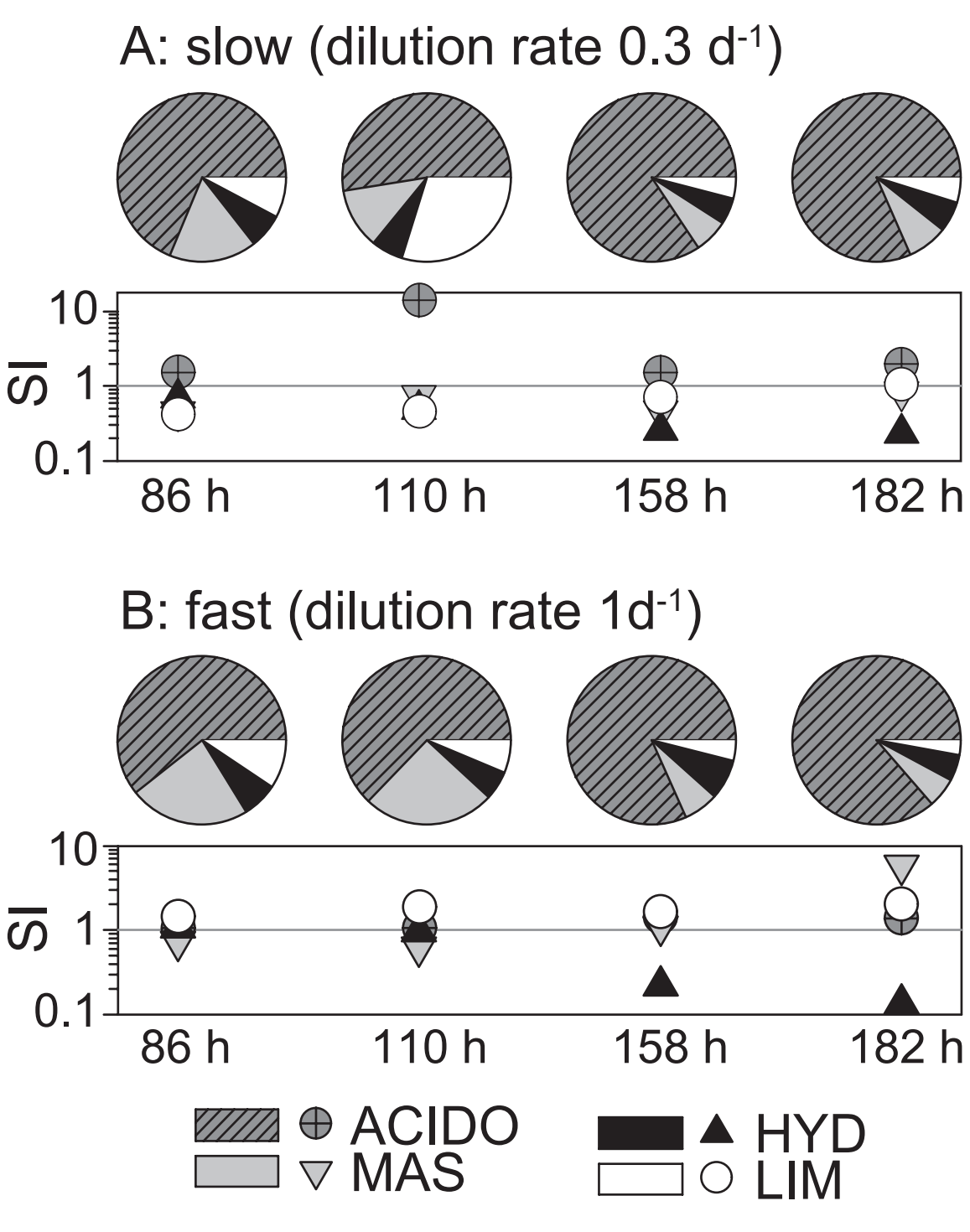
A: slow (dilution rate 0.3 d-1)
10
1
0.1
SI
86 h
110 h
158 h
182 h
B: fast (dilution rate 1d-1)
10
1
0.1
SI
86 h
110 h
158 h
182 h
ACIDO
MAS
HYD
LIM

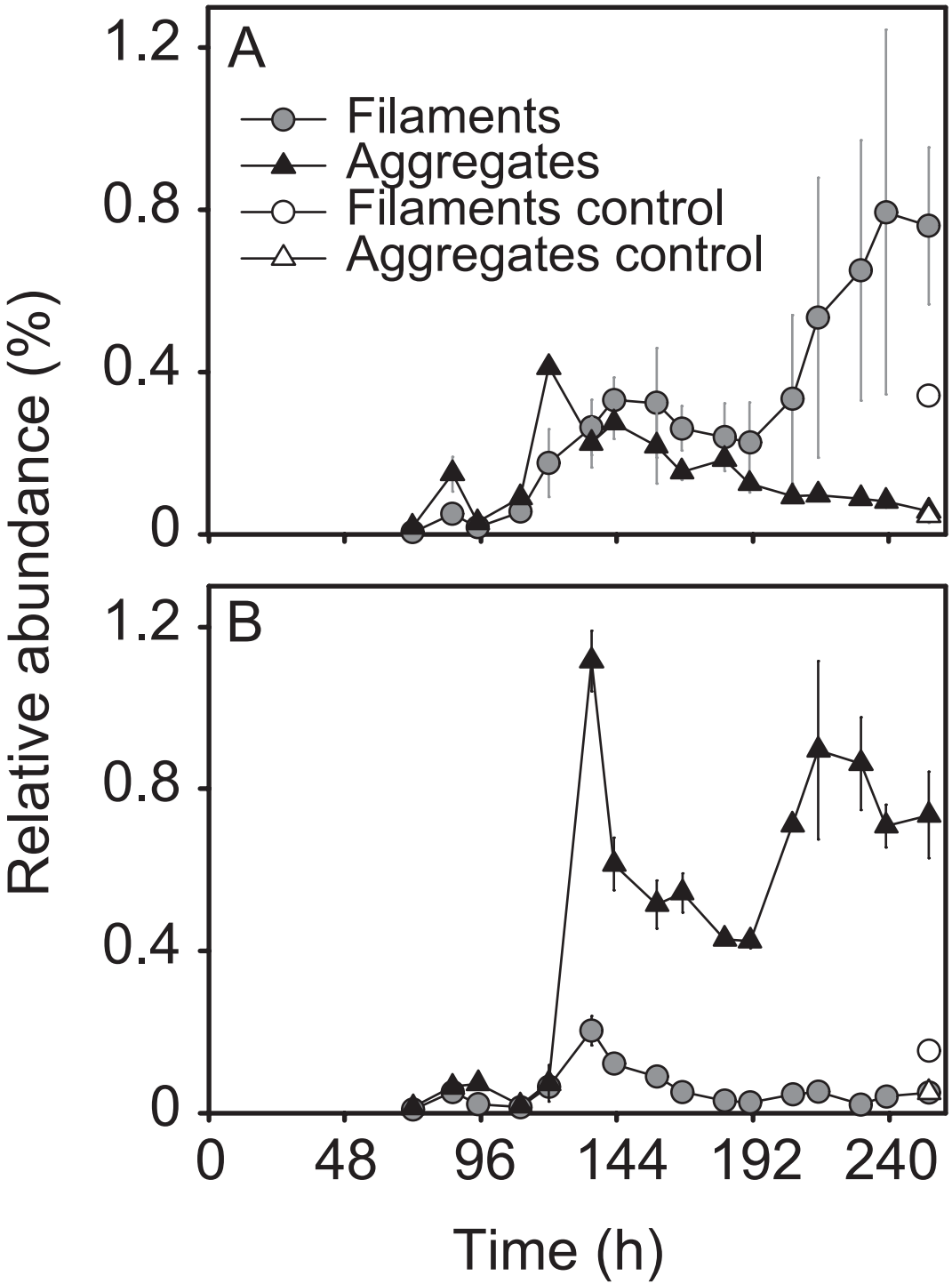
A
B
Filaments
Aggregates
Filaments control
Aggregates control
Relative abundance (%)
Time (h)
0
0.4
0.8
1.2
0
48
96
144
192
240

Supplementary data to Salcher et al.

Table S1. Student's t-test results of comparisons of cell densities of bacterial strains between the different treatments.

Table S2. Student's t-test results of comparisons of growth rates of bacterial strains between the different treatments.

Table S3. Metabolic characteristics of the four bacterial strains.

Figure S1. Bootstrapped maximum likelihood tree of the 16S rDNA of the bacterial strains and their closest relatives.

Figure S2. Schematic overview of the continuous cultivation system.

Figure S3. Total microbial cell densities, bacterial biomass, and growth and loss rates.

Figure S4: Substrate partitioning between the four strains.

Figure S5. Microphotographs of the flagellate *P. malhamensis* with ingested bacteria in food vacuoles.

Figure S6. Total grazing rates of *P. malhamensis* on individual bacterial strains.

Figure S7. Microphotographs of bacterial morphotypes.

Figure S8. Schematic overview or the outcome of our experiments.

Table S1. Student's t-test results of comparisons of cell densities of bacterial strains between the different treatments. Only significant differences are displayed.

Treatment	Total	ACIDO	MAS	HYD	LIM
monocult. vs. co-cult. slow	-9.46***	-8.30***	-16.70***	19.12***	n.s.
monocult. vs. co-cult. fast	-5.01***	-5.56**	-10.19***	6.67**	n.s.
co-cult. slow vs. co-cult. fast	n.s.	-3.28*	n.s.	n.s.	n.s.
grazing slow vs. grazing fast	n.s.	n.s.	7.98*	n.s.	n.s.

***, p<0.001; **, p<0.01; *, p<0.05; n.s., not significant

Table S2. Student's t-test results of comparisons of growth rates of bacterial strains between the different treatments. Only significant differences are displayed.

Treatment	Total	ACIDO	MAS	HYD	LIM
monocult. vs. co-cult. slow	-13.42***	-3.46*	-13.44***	7.31**	n.s.
monocult. vs. co-cult. fast	-19.87***	-5.47**	-12.53***	n.s.	n.s.
co-cult. slow vs. co-cult. fast	4.44*	n.s	2.97*	n.s.	n.s.

***, p<0.001; **, p<0.01; *, p<0.05; n.s., not significant

Table S3. Metabolic characteristics of the four bacterial strains. A biomass increase or decrease is given in % normalized to the control treatment (ALW without carbon source) and was scored as highly positive (++, >180% compared to control treatments, dark green), positive (+, 50 - 180% compared to control, green), weak (w, 10 – 50% compared to control, light green), no growth (0, -20 – 10% compared to control, grey), and inhibited (-, <-20% compared to control, red). The panel on the bottom gives an overview on the number of substrates scored as ++, +, w, 0, and – of individual bacterial strains.

	Acidovorax MMS1-28	*Massilia* MMS1-16	*Hydrogenop.* EECy4	*L. planktoni.* II-D5
Amino acids				
D-Alanine	15	228	34	-6
L-Alanine	199	201	93	9
L-Asparagine	138	126	-17	-7
D-Aspartic Acid	162	-3	-17	-7
L-Aspartic Acid	160	167	57	21
L-Glutamine	100	211	57	-4
L-Glutamic Acid	198	173	101	30
L-Proline	245	161	113	53
D-Serine	-20	-9	-22	23
L-Serine	52	223	-7	2
D-Threonine	-19	-6	-14	-17
L-Threonine	52	277	21	13
Amino sugars				
N-Acetyl-D-Glucosamine	16	13	-7	-3
N-Acetyl-β-D-Mannosamine	23	19	1	21
D-Glucosaminic Acid	-17	-1	185	-10
Carboxylic acids				
Acetic Acid	59	86	62	16
Acetoacetic Acid	28	8	-1	0
Bromo Succinic Acid	84	63	4	-12
Citric Acid	-22	74	-18	-11
Fumaric Acid	181	46	-19	-13
Formic Acid	1	-1	-19	84
Glycolic Acid	26	-6	25	-6
Glyoxylic Acid	-9	-7	310	-7
α-Hydroxy Butyric Acid	45	21	7	14
α-Hydroxy Glutaric Acid-γ-Lactone	-7	4	3	251
p-Hydroxy Phenyl Acetic Acid	108	-6	76	-13
m-Hydroxy Phenyl Acetic Acid	-20	-7	110	-10
α-Keto-Butyric Acid	43	40	-19	1
α-Keto-Glutaric Acid	70	2	-14	30
L-Lactic Acid	164	0	35	34
D-Gluconic Acid	181	3	107	9
D, L-Malic Acid	108	74	183	-11
D-Malic Acid	54	146	39	2
L-Malic Acid	118	63	-19	-5
Methyl Pyruvate	30	148	93	20

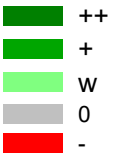

	Acidovorax MMS1-28	*Massilia* MMS1-16	*Hydrogenop.* EECy4	*L. planktoni.* II-D5
Mono Methyl Succinate	72	25	115	11
Propionic Acid	8	85	-24	-13
Pyruvic Acid	75	162	111	-5
D-Saccharic Acid	47	11	103	0
Succinic Acid	120	155	49	4
Tricarballylic Acid	30	2	-3	-10
Dipeptides				
L-Alanyl-Glycine	28	45	0	15
Glycyl-L-Aspartic Acid	-19	11	51	-6
Glycyl-L-Glutamic Acid	52	161	-7	7
Glycyl-L-Proline	-20	154	-23	-8
Glycols				
Tween 20	140	87	34	-13
Tween 40	127	92	26	-10
Tween 80	62	60	5	-5
1,2-Propanediol	-12	1	-12	2
Glycosides				
α-Methyl-D-Galactoside	0	2	-14	29
α-Methyl-D-Glucoside	8	16	9	14
Monosaccharides				
L-Arabinose	84	333	-7	17
L-Fucose	-11	-3	-15	-9
D-Fructose	141	189	-22	39
D-Galactose	248	4	-12	7
α-D-Glucose	238	112	225	33
L-Lyxose	-14	4	-20	-7
D-Mannose	190	322	-6	37
D-Psicose	-15	-4	14	-13
L-Rhamnose	3	-2	-19	0
D-Ribose	4	-1	4	13
D-Xylose	-9	1	-19	11
Oligosaccharides				
D-Cellobiose	-11	216	-16	10
α-D-Lactose	86	2	-20	20
Lactulose	-7	0	-17	22
Maltose	5	224	-23	15
Maltotriose	4	235	3	11
D-Melibiose	49	4	17	28
Sucrose	-10	-2	160	28
D-Trehalose	22	24	-5	38
Ribonucleosides				
Adenosine	-11	91	-6	-18
Inosine	-17	90	-25	-13
Uridine	-6	20	-21	13
Deoxyribonucleosides				
2-Deoxy Adenosine	22	18	83	7
Thymidine	-10	-7	-22	8

	Acidovorax MMS1-28	*Massilia* MMS1-16	*Hydrogenop.* EECy4	*L. planktoni.* II-D5
Sugar acids				
D-Glucuronic Acid	-6	0	-17	-3
Glycerol	107	-1	44	-7
M-Inositol	-19	-1	-18	-10
D-Mannitol	174	-1	-18	23
D-Sorbitol	138	-2	-16	-7
L-Galactonic Acid-γ-Lactone	-12	-7	37	3
D-Galactonic Acid-γ-Lactone	-16	-4	-15	15
D-Galacturonic Acid	-14	187	-22	-2
Mucic Acid	28	-4	99	-3
M-Tartaric Acid	41	14	-10	-5
Adonitol	20	19	98	5
Dulcitol	29	41	15	33
Amides				
Glucuronamide	-16	-2	-20	7
Amines				
Phenylethylamine	13	-7	-23	-12
2-Aminoethanol	-10	-6	-22	-7
Tyramine	-3	-7	-24	-16
Sugar phosphates				
D-Fructose-6-Phosphate	1	12	-11	8
D-Glucose-1-Phosphate	-13	26	245	-8
D-Glucose-6-Phosphate	-20	-6	4	-6
D,L-α-Glycerol-Phosphate	-4	-1	-17	16

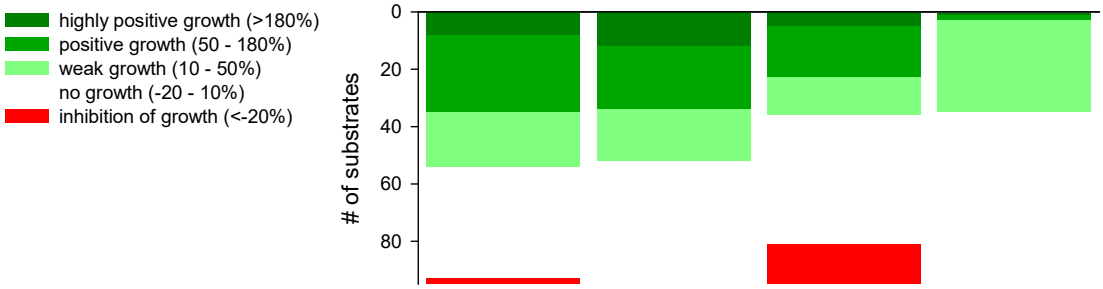

Figure S1. Bootstrapped maximum likelihood tree of the 16S rDNA of the bacterial strains and their closest relatives. Nodes with bootstrap supports <40% were collapsed to multifurcations. The strains used in the experiments are marked in bold. The scale bar at the bottom represents 10% sequence divergence.

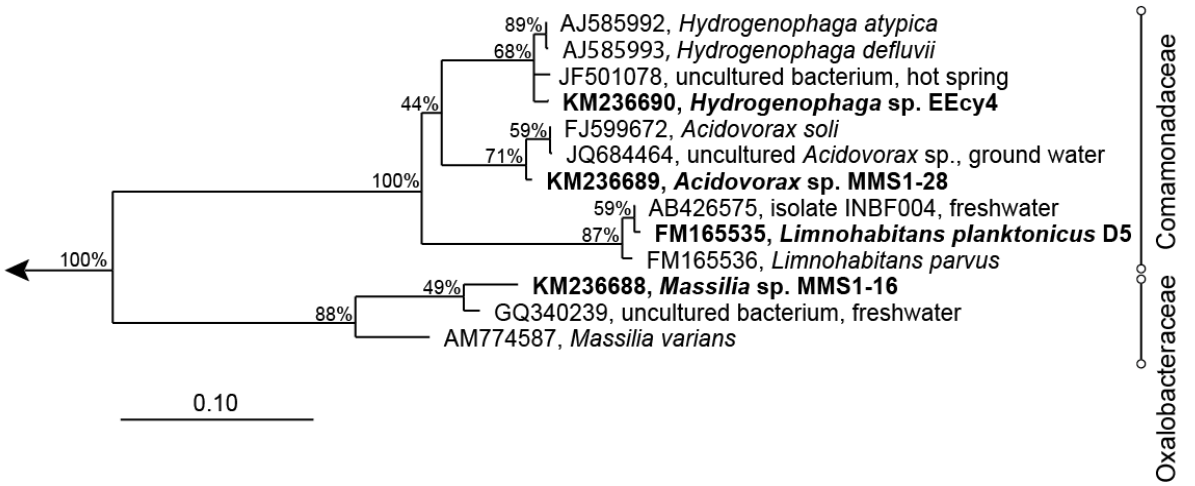

Figure S2. Schematic overview of the continuous cultivation system. Two different flow rates of medium to the cultivation vessels were used to modulate the assumed slow (S, 0.3 d^{-1}) and fast (F, 1 d^{-1}) growth of microbes, respectively. The four bacterial strains were inoculated in equal initial numbers to all vessels. *Poterioochromonas malhamensis* DS was added to vessels S2, S3, F2, and F3 after 72 h, while vessels S1 and F1 served as control treatments without protists. Abbreviations: mv, medium vessel; pp, peristaltic pump; ap, air pump; av, aeration valve; bt, bacterial trap; af, air filter, cv, cultivation vessel; ov; overflow vessel.

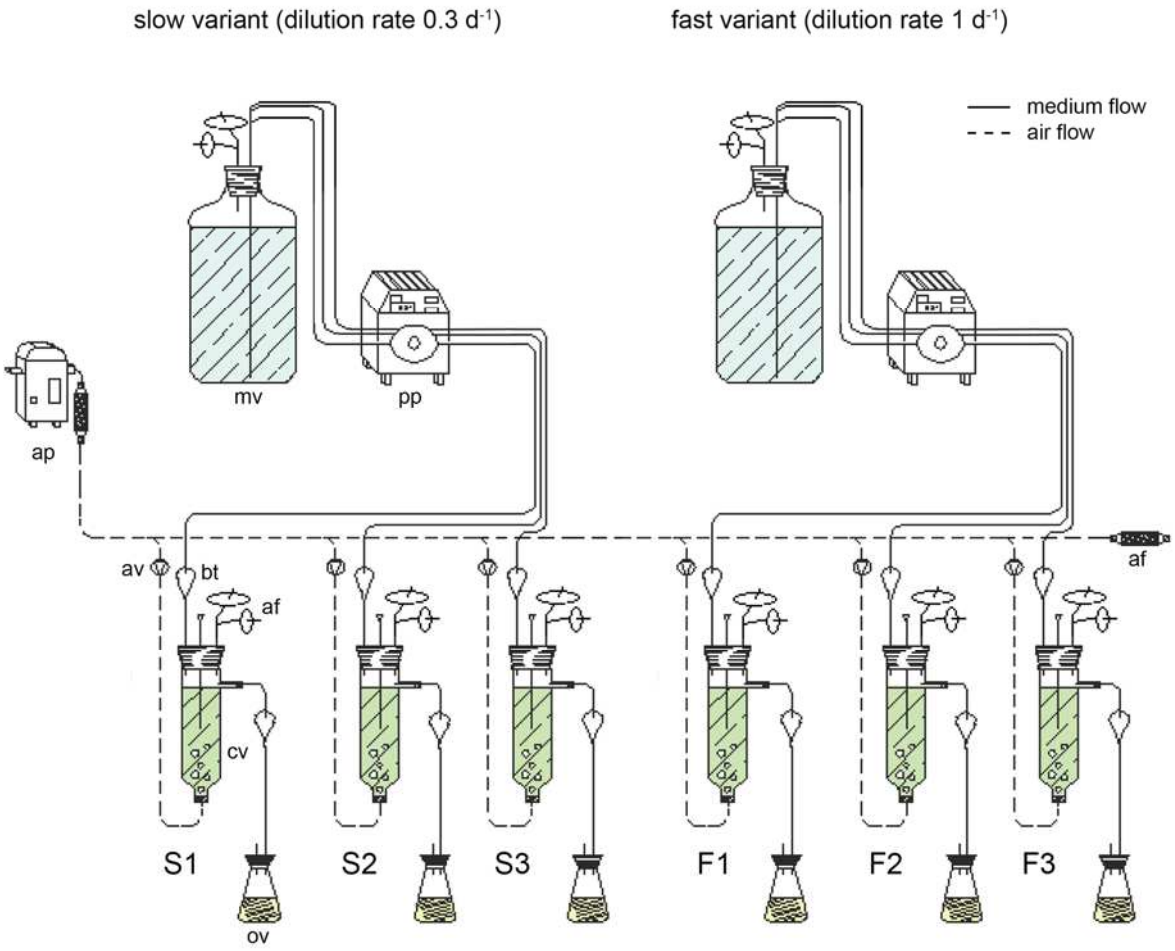

Figure S3. Total microbial cell densities, bacterial biomass, and growth and loss rates. A: Accumulated numbers of the four strains cultivated in batch cultures. B, C: Total numbers of bacteria and flagellates in the slow and fast variants of the chemostat. D, E: Total bacterial biomass in the slow and fast variants of the chemostat. F, G: Growth and loss rates of all bacteria (until t_{182} h) in the slow and fast variants of the chemostat.

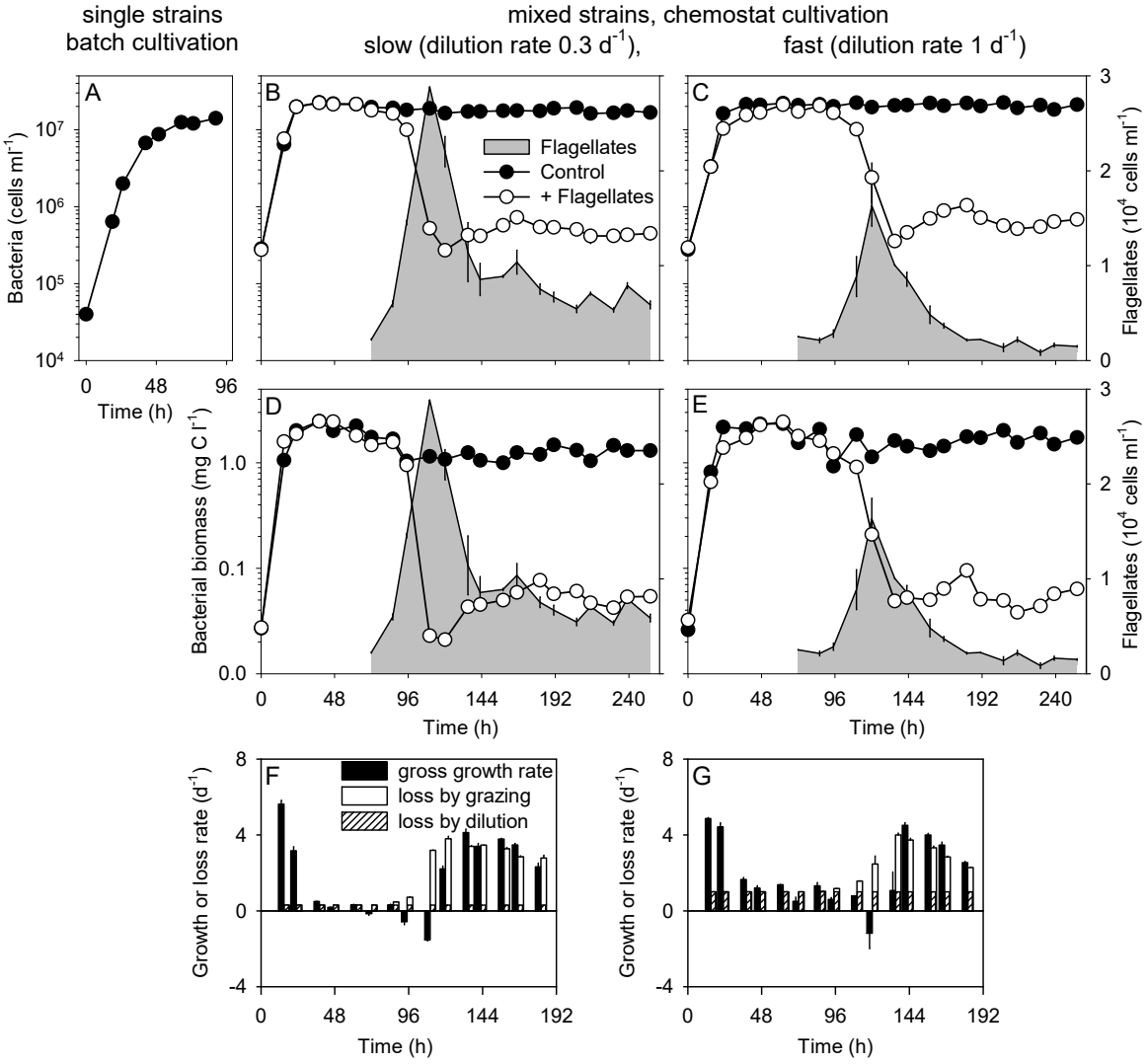

Figure S4: Substrate partitioning between the four strains. A: Number of shared substrates that supported the growth of the four strains. B: Agglomerative hierarchical clustering of the four strains based on similarities in their substrate uptake patterns (unweighted pair-group average of Pearson's correlation coefficient). The dotted line indicates the level of significance. ACIDO, *Acidovorax* sp. MMS1-28; MAS, *Massilia* sp. MMS1-16; HYD, *Hydrogenophaga* sp. EECy4; LIM, *Limnohabitans planktonicus* II-D5^{T}.

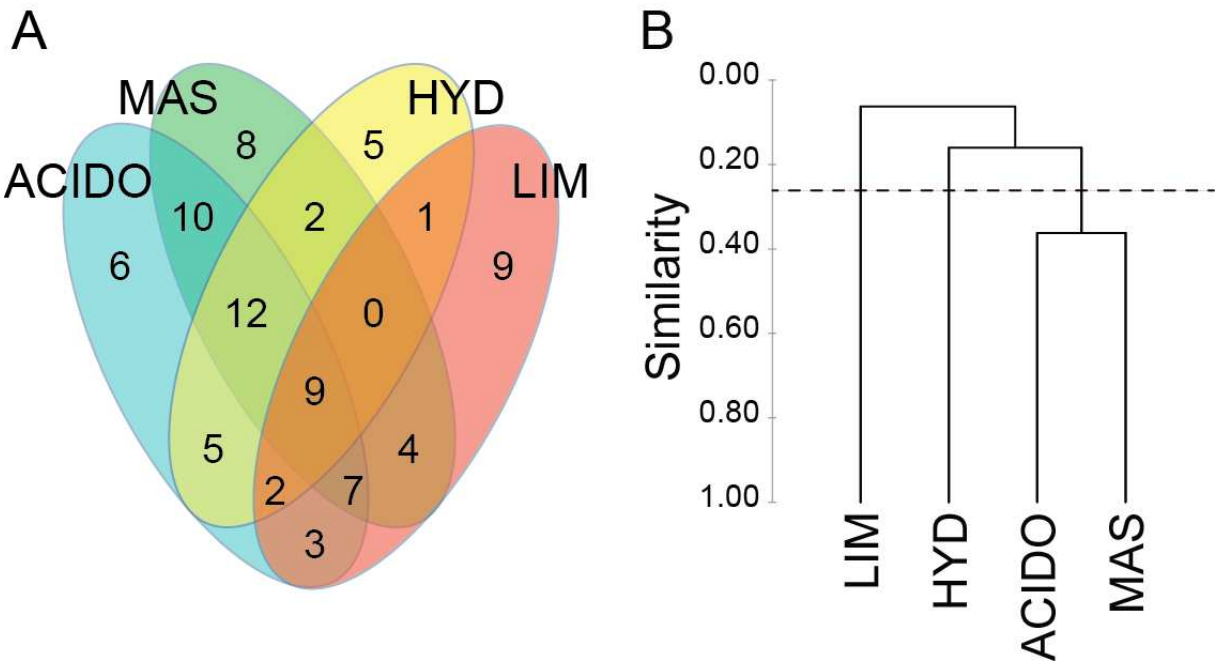

Figure S5. Microphotographs of the flagellate *P. malhamensis* with ingested bacteria in food vacuoles. A-C: *Acidovorax* sp. MMS1-28; D: *Massilia* sp. MMS1-16; E-F: L. *planktonicus* II-D5^{T}; G: *Hydrogenophaga* sp. EECy4. The scale bar in A applies to all pictures.

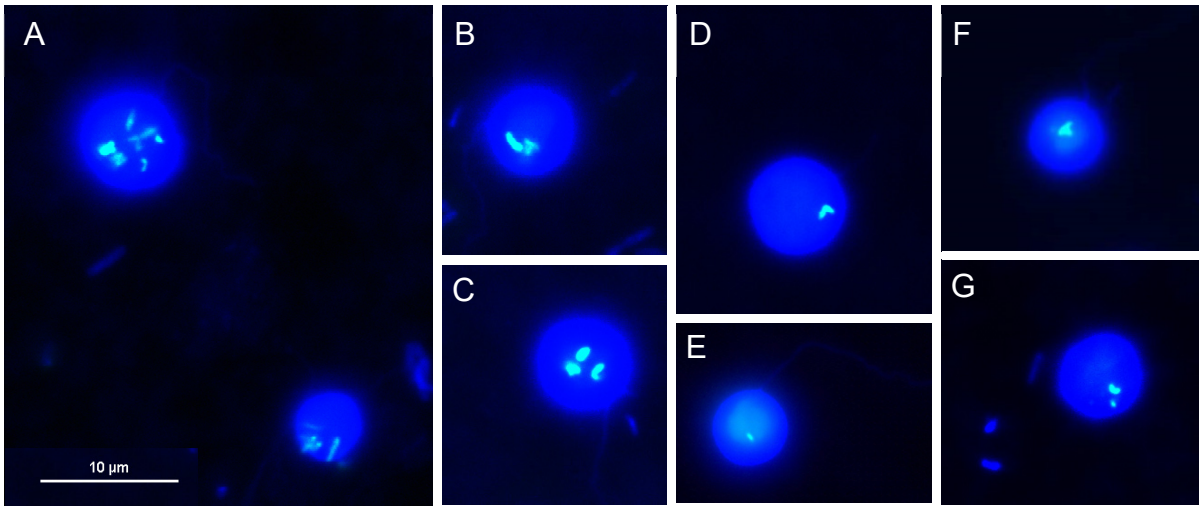

Figure S6. Total grazing rates of *P. malhamensis* on individual bacterial strains in the slow (A) and fast (B) variants of the chemostat. ACIDO, *Acidovorax* sp. MMS1-28; MAS, *Massilia* sp. MMS1-16; HYD, *Hydrogenophaga* sp. EECy4; LIM, *Limnohabitans planktonicus* II-D5^{T}.

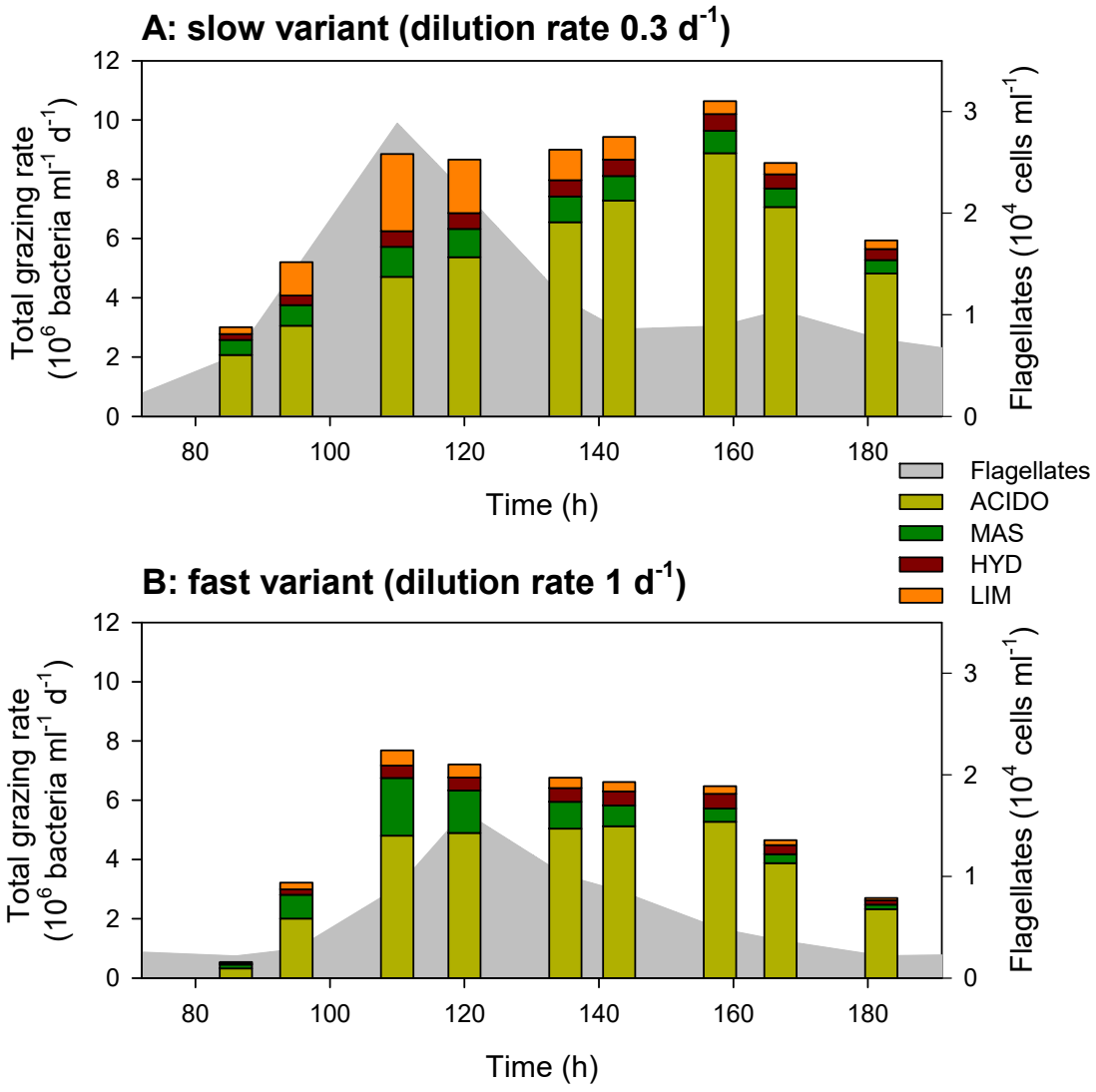

Figure S7. Microphotographs of bacterial morphotypes. A-C: filamentous bacteria affiliated with *Massilia* sp. MMS1-16 (green, A, C) or *Acidovorax* sp. MMS1-28 (red, B) in the slow variants. D-F: aggregates affiliated with *Acidovorax* sp. MMS1-28 (red, D, E) or *Hydrogenophaga* sp. EECy4 (blue, E, red, F). The scale bar in C and F applies to all pictures.

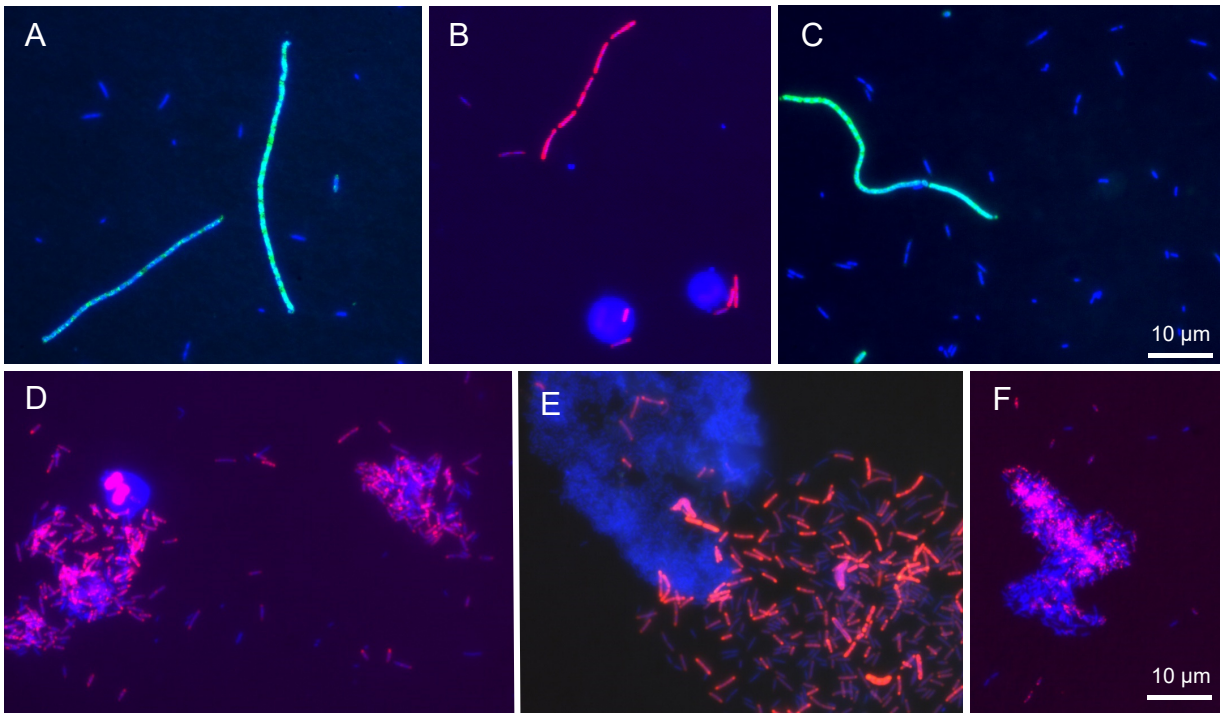

Figure S8. Schematic overview or the outcome of our experiments. The different strains are displayed in light green (*Acidovorax* sp. MMS1-28), dark green (*Massilia* sp. MMS1-16), brown (*Hydrogenophaga* sp. EECy4), and orange (L*. planktonicus* II-D5^{T}). The schematic graphs represent abundance data taken from Figure 1. Only the fast variant of the experimental setup is displayed for reasons of simplicity.